Repeatability and Reproducibility of Manual Choroidal Volume Measurements Using Enhanced Depth Imaging Optical Coherence Tomography

Jay Chhablani, Giulio Barteselli, Haiyan Wang, Sharif El-Emam, Igor Kozak, Aubrey L. Doede, Dirk-Uwe Bartsch, Lingyun Cheng, and William R. Freeman

Purpose. To evaluate the repeatability and reproducibility of manual choroidal volume (CV) measurements by spectral domain- optical coherence tomography (SD-OCT) using enhanced depth imaging (EDI).

Methods. Sixty eyes of 32 patients with or without any ocular chorioretinal diseases were enrolled prospectively. Thirty-one choroidal scans were performed on each eye, centered at the fovea, using a raster protocol. Two masked observers demarcated choroidal boundaries by using built-in automated retinal segmentation software on two separate sessions. Observers were masked to each other's and their own previous readings. A standardized grid centered on the fovea was positioned automatically by OCT software, and values for average CVs and total CVs in three concentric rings were noted. The agreement between the intraobserver measurements or interobserver measurements was assessed using the concordance correlation coefficient (CCC). Bland-Altman plots were used to assess the clinically relevant magnitude of differences between inter- and intraobserver measurements.

Results. The interobserver CCC for the overall average CV was very high, 0.9956 (95% confidence interval [CI], 0.991–0.9968). CCCs for all three Early Treatment Diabetic Retinopathy Study concentric rings between two graders was 0.98 to 0.99 (95% CI, 0.97–0.98). Similarly intraobserver repeatability of two graders also ranged from 0.98 to 0.99. The interobserver coefficient of reproducibility was approximately 0.42 (95% CI, 0.34–0.5 mm^3) for the average CV.

Conclusions. CV measurement by manual segmentation using built-in automated retinal segmentation software on EDI-SD-OCT is highly reproducible and repeatable and has a very small range of variability. (*Invest Ophthalmol Vis Sci.* 2012;53:2274–2280) DOI:10.1167/iovs.12-9435

From the Jacobs Retina Center at Shiley Eye Center, University of California, San Diego, La Jolla, California.

Supported by an unrestricted research fund from the Jacobs Retina Center at Shiley Eye Center, University of California, San Diego (LC), and by National Institutes of Health-EY grants 007366 (WRF), 020617 (LC), 018589 (WRF), and 016323 (DUB).

Submitted for publication January 5, 2012; revised February 23 and 26, 2012; accepted February 27, 2012.

Disclosure: **J. Chhablani**, None; **G. Barteselli**, None; **H. Wang**, None; **S. El-Emam**, None; **I. Kozak**, None; **A.L. Doede**, None; **D.-U. Bartsch**, None; **L. Cheng**, None; **W.R. Freeman**, None

Corresponding author: William R. Freeman, MD, Jacobs Retina Center at Shiley Eye Center, University of California, San Diego, 9415 Campus Point Drive, MC 0946, La Jolla, CA 92093-0946; wrfreeman@ucsd.edu.

The choroid plays an important role in providing oxygen and nutrition to the outer retinal layers. It is a primary site of involvement in various chorioretinal diseases such as central serous chorioretinopathy (CSR), choroidal neovascularization, polypoidal choroidal vasculopathy (PCV), Vogt-Koyanagi-Harada (VKH) disease, and other chorioretinal inflammatory disorders. In CSR, the primary pathology is choroidal vascular hyperpermeability.[1] PCV presents with multiple serosanguinous pigment epithelial detachments due to choroidal polyps, confirmed with histopathology.[2] The choroid is secondarily involved in VKH disease and chorioretinal inflammatory disorders. In VKH disease, choriocapillaris involvement was shown on histopathologic examination.[3] Thus, evaluation of the choroid would be helpful to understand the pathophysiology, diagnosis, and management of chorioretinal disorders.

Indocyanine green (ICG) angiography is useful for evaluating choroidal vascular diseases.[4] Ultrasonography is used for quantitative assessment of choroidal thickness[5] but is unable to provide reliable and repeatable measurements due to sampling error. With the advent of high-resolution spectral domain-optical coherence tomography (SD-OCT), enhanced depth choroidal imaging (EDI) is now possible. EDI of Spectralis OCT (Heidelberg Engineering, Heidelberg, Germany) helps to obtain a good quality image of the choroid by moving the sensitivity curve at the sclera.[6] Image averaging, eye tracking, high-speed scanning, and low speckle noise produce high-quality choroid images with EDI-OCT Spectralis OCT.

Choroidal thickness has been measured using EDI. Recent reports have shown high reproducibility of choroidal thickness measurements by using various SD-OCT instruments on normal subjects. Choroidal thickness in different pathologies such as neovascular age-related macular degeneration (decreased choroidal thickness),[7,8] high myopia (decreased choroidal thickness),[9] CSR (increased choroidal thickness),[10] PCV (increased choroidal thickness),[7,8] white dot syndrome (increased choroidal thickness),[11] and VKH disease (increased choroidal thickness),[12,13] have been reported.

Those studies performed thickness measurement only in selected, usually subfoveal, points of the macula. Measurements taken at multiple single points could be misleading in the overall assessment of choroidal involvement by the disease. Volumetric analysis of the choroid in chorioretinal diseases would be helpful to assess the disease course and response to treatment.

In contrast to retinal imaging, automated choroidal segmentation algorithm software is not presently available. Thus, choroidal segmentation must be performed manually, and it is essential to estimate the error of the manual segmentation in order to distinguish clinical change from measurement variability.

This study describes a novel technique for manual choroidal segmentation using built-in automated retinal segmentation

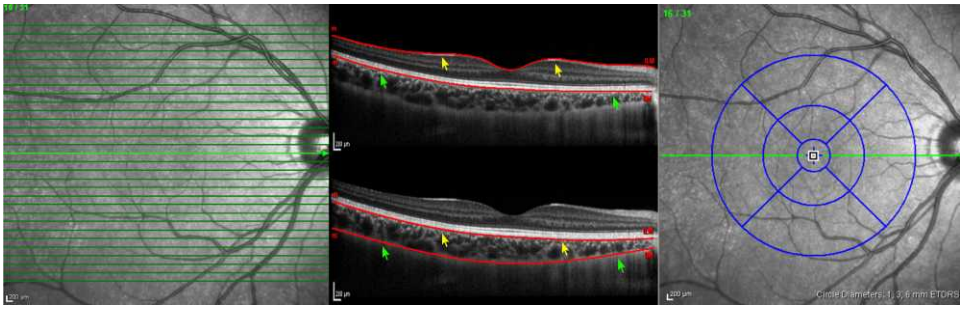

Figure 1. EDI SD-OCT raster scan protocol (*left*), automated retinal segmentation (*middle top*), manual choroidal segmentation (*middle bottom*), and standardized grid (*right*) including three concentric rings with a total of nine subfields centered on the fovea. Internal limiting membrane line (*yellow arrows*) and basement membrane line (*green arrows*) on automated retinal segmentation was moved to the base of retinal pigment epithelium (*yellow arrows*) and chorioscleral interface (*green arrows*) to demarcate choroidal boundaries (*middle bottom*).

software with EDI-OCT using Spectralis OCT to obtain the choroidal volume measurements over standardized circles. The aim of the present study was to evaluate the reproducibility and repeatability of choroidal volume measurements by a manual choroidal segmentation technique using concordance correlation coefficient (CCC) and coefficients of reproducibility and repeatability.

Methods

For this prospective study, 60 eyes of 32 patients with or without ocular chorioretinal disease were consecutively included. Written informed consent for diagnostic procedures was obtained from each subject before examination. The study was approved by the Institutional Review Board at Shiley Eye Center at the University of California San Diego and was conducted in adherence to the tenets of the Declaration of Helsinki. After pupils were dilated with tropicamide 1% and phenylephrine 2.5%, all OCT scans were performed by a single retina specialist who is experienced at performing scans using EDI-Spectralis OCT. Spectralis OCT provides up to 40,000 A scans/sec with a depth resolution of 7 μm in tissue and a transversal resolution of 14 μm by using a superluminescence diode with an 870-nm bandwidth. Raster scans with any single poor choroidal scan were excluded. Two experienced retina specialists (GB and JC) analyzed all scans in two separate sessions.

Choroidal Volume Imaging Protocol

Raster imaging consisting of 31 high-resolution B scans was performed with each eye, centered on the fovea. An internal fixation light was used to center the scanning area on the fovea. Each scan was 9.0 mm in length and spaced 240 μm apart from each other. Single OCT images consisting of 512 A lines were acquired in 0.78 ms. All 31 OCT macular B scans were acquired in a continuous, automated sequence and covered a 30° × 25° area centered on the fovea (Fig. 1). The scans were obtained for analysis after 25 frames were averaged using built-in automatic averaging software (TruTrack; Heidelberg Engineering, Heidelberg, Germany) to obtain a good-quality choroidal image.

Choroidal Image Analysis

Choroidal segmentation was performed manually after the automated retinal layer segmentation software was disabled. Masked observers moved the reference lines of the built-in automated segmentation from the retinal boundaries to the choroidal boundaries. The internal limiting membrane line was moved to the outer part of the hyper-reflective line corresponding to the base of the retinal pigment epithelium. The basement membrane line, which is the reference line for the posterior edge of the retina, was moved to the posterior edge of the choroid as demarcated by the hyper-reflective margin line corresponding to the chorioscleral interface (Fig. 1). This method allowed us to use the automatic retinal thickness/volume map features of the built-in software. The automated software allowed choroidal volume calculations to be made in the manner similar to that for retinal volume analysis.

The standardized grid[14] was positioned automatically by the Spectralis OCT software and was visualized in a software designed to map macular thickness (Fig. 1). The standardized grid divided the macula into three circles diameters of 1 mm (central), 3 mm (inner), and 6 mm (outer). Values for overall average choroidal volume and total choroidal volume in each circle of standardized grid were noted.

Statistical Analysis

Two retina specialists (GB [Observer 1] and JC [Observer 2]) performed manual choroidal segmentation on choroidal raster scans of each eye on two different occasions. They were masked as to their previous measurements and to each other's measurements. In this manner, a total of 120 choroidal volume scans were compared for interobserver reproducibility. For intraobserver repeatability, 60 choroidal volume scans from each observer were analyzed. Inter- and intraobserver agreement was evaluated for overall average and total

Table 1. Summary of Mean Differences between Two Observers, Limits of Agreement, Correlation Coefficient, and Coefficient of Reproducibility for Interobserver Variability

Area	Mean CV 1 (mm^3)	Mean CV 2 (mm^3)	SE (mm^3)	Difference between Means (mm^3)	95% Limit of Agreement* (mm^3)	CCC	CR (mm^3)	95% CI (mm^3)
Average	8.74	8.63	0.007	+0.0232	−0.4 to +0.44	0.9956	0.42	0.34–0.5
Central ring	0.29	0.28	0.0006	+0.0007	−0.024 to +0.025	0.9880	0.024	0.02–0.03
Inner ring	2.04	2.045	0.0003	+0.0038	−0.107 to +0.11	0.9953	0.11	0.09–0.13
Outer ring	6.8	6.37	0.027	−0.019	−0.42 to +0.38	0.9923	0.4	0.32–0.47

CR, coefficient of reproducibility; Mean CV 1, choroidal volume measurements obtained by Observer 1; Mean CV 2, choroidal volume measurements obtained by Observer 2.

*95% limits of agreement = mean difference ±1.96 × SD.

Table 2. Summary of Mean Differences, Limits of Agreement, Correlation Coefficient, and Coefficient of Repeatability for Intraobserver Variability for Observer 1

Area	Mean CV 1 (mm^3)	Mean CV 2 (mm^3)	SE (mm^3)	Difference between Means (mm^3)	95% Limit of Agreement* (mm^3)	CCC	CR (mm^3)	95% CI (mm^3)
Average	8.79	8.67	0.007	−0.043	−0.46 to +0.37	0.9955	0.42	0.31–0.52
Central ring	0.29	0.285	0.01	+0.0003	−0.014 to +0.015	0.9956	0.014	0.011–0.019
Inner ring	2.095	2.0450	0.0045	−0.013	−0.12 to +0.09	0.9956	0.11	0.078–0.132
Outer ring	6.9	6.3250	0.0045	−0.025	−0.49 to +0.44	0.9891	0.47	0.34–0.58

CR, coefficient of reproducibility; Mean CV 1, choroidal volume measurements obtained by Observer 1; Mean CV 2, choroidal volume measurements obtained by Observer 2.

*95% limits of agreement = mean difference ±1.96 × SD.

choroidal volume at three concentric rings of a standardized grid with diameters of 1, 3, and 6 mm.

Agreement between intraobserver measurements or interobserver measurements was assessed using the CCC. Bland-Altman plots were used to assess the clinically relevant magnitude of the differences between the measurements and observers.[15]

Results

This prospective study included 60 eyes of 32 subjects. The mean age of the 32 subjects was 44 years (range, 31–84 years) with 15 men and 17 women. The racial distribution included Caucasians (26 subjects), Asians (4 subjects), and Hispanics (2 subjects). Disease distribution among subjects included no ocular disease (40 eyes), high myopia (4 eyes), epiretinal membrane (5 eyes), and dry macular degeneration (11 eyes).

The interobserver CCC for overall average choroidal volume was 0.9956 (95% confidence interval [CI], 0.991–0.9968). The CCC for all three standardized concentric rings between two graders was 0.98 to 0.99 (95% CI, 0.97–0.98). Similarly, intraobserver repeatability of two graders was also 0.98 to 0.99. Intra- and interobserver correlation coefficient and differences between means for average choroidal volume and choroidal volume at three concentric rings are shown in Tables 1, 2, and 3. Table 4 shows mean choroidal thickness and SEM measurements in various locations with standardized grids at posterior poles.

The interobserver coefficient of reproducibility was approximately 0.25 (95% CI, 0.2–0.3 mm^3) for the average choroidal volume. The mean (±SD) difference in average choroidal volume measurements between the two observers was 0.11 mm^3 (±0.12 mm^3). Coefficients of repeatability and reproducibility for each ring, for intraobserver and interobserver, respectively, are shown in Tables 1, 2, and 3. Bland-Altman plots of differences between mean choroidal volumes from the two observers' measurements of average and of each ring are shown in Figures 2, 3, and 4.

Discussion

Before the introduction of ICG angiography, ultrasonography was used to assess the choroidal thickness, albeit with low reproducibility. ICG angiography contributed significantly to the understanding of chorioretinal disease,[4] but reproducible quantitative assessment of the choroid in vivo was still lacking. With the advent of enhanced depth OCT imaging, quantitative assessment of the choroid in vivo is now possible. Recently, reports have been published regarding the reproducibility of choroidal thickness using enhanced depth SD-OCT or long-wavelength OCT devices.[12,13,16,17] These studies report choroidal thickness at a single point or at a small number of points on vertical scans and horizontal scans. Quantitative assessment of overall choroidal anatomy, including volume at the posterior pole choroid and topographic maps of this vascular bed, may be more useful in providing insight into macular disease.

To address this issue, we report a novel technique of manual choroidal segmentation of the choroid by using built-in automated retinal segmentation software with EDI, using the Spectralis OCT. We used EDI and eye-tracking functions to obtain good quality and reproducibility of 31 choroidal scans in a raster protocol. Image stabilization with colocalization to a simultaneous infrared scanning laser ophthalmoscope OCT imaging is likely one of the factors for the high repeatability that we found. We used segmentation software originally designed to determine retinal borders to demarcate the choroid and obtained the choroidal volume measurements by using the same automated software. Manual demarcation of choroidal borders is a tedious process, and for that reason, we also performed a pilot study (unpublished data) of 20 eyes to assess the effect of scanning density on choroidal volume calculation and found no statistically significant difference in choroidal volume measurements after manual segmentation of every scan compared to 31 raster protocol scans. Therefore, in the present study, we analyzed reproducibility of the choroidal volume measurement for alternate scan segmentation. To our knowledge, there are no previous studies reporting choroidal

Table 3. Summary of Mean Differences, Limits of Agreement, Correlation Coefficient, and Coefficient of Repeatability for Intraobserver Variability for Observer 2

Area	Mean CV 1 (mm^3)	Mean CV 2 (mm^3)	SE (mm^3)	Difference between Means (mm^3)	95% Limit of Agreement* (mm^3)	CCC	CR (mm^3)	95% CI (mm^3)
Average	8.69	8.79	0.009	−0.09	−0.28 to +0.1	0.9983	0.19	0.14–0.24
Central ring	0.275	0.2754	0.00003	−0.004	−0.02 to +0.012	0.9938	0.016	0.011–0.02
Inner ring	2.04	2.06	0.001	−0.026	−0.098 to +0.044	0.9971	0.07	0.05–0.09
Outer ring	6.3	6.45	0.013	−0.06	−0.205 to +0.084	0.9983	0.14	0.11–0.18

CR, coefficient of reproducibility; Mean CV 1, choroidal volume measurements obtained by Observer 1; Mean CV 2, choroidal volume measurements obtained by Observer 2.

*95% limits of agreement = mean difference ±1.96 × SD.

Table 4. Mean Choroidal Thickness and SEM in Various Locations on Standardized Grid at Posterior Pole

Area	Mean CT 1 (μm)	Mean CT 2 (μm)	SEM (μm)
Central ring	264.15	263.83	1.18
Inner superior quadrant	271.13	268.7	0.82
Inner nasal quadrant	239.12	238.5	0.95
Inner inferior quadrant	246.5	245.76	0.99
Inner temporal quadrant	264.74	262.65	0.73
Outer superior quadrant	269.42	271.5	0.73
Outer nasal quadrant	183.38	185.02	0.70
Outer inferior quadrant	235.13	234.08	0.57
Outer temporal quadrant	247.28	244.62	0.73

Mean CT 1, choroidal thickness measurements obtained by Observer 1; Mean CT 2, choroidal thickness measurements obtained by Observer 2.

volume measurement with the Spectralis OCT instrument, using manual segmentation in EDI mode.

Our study showed a very high reproducibility ($r = 0.98$–0.99) in all three concentric rings of standardized study areas. With the help of EDI software, the demarcation line of chorioscleral border was distinctly seen, especially after averaging. In this study, interobserver and intraobserver coefficients of reproducibility were 0.25 and 0.050. to 47 mm^3 for average choroidal volume measurements, respectively. We found good interobserver and intraobserver reproducibility especially in the central ring (1-mm diameter) of Early Treatment Diabetic Retinopathy Study areas. The outer ring (3-mm diameter) showed relatively lower reproducibility and repeatability than those of the other two rings but not significantly different. The cause of this comparatively low reproducibility could be poor delineation of the choroid in the peripheral part of the scan. Nonetheless, the intraobserver repeatability in the outer circle was excellent ($r = 0.98$).

There have been several reports of foveal choroidal thickness reproducibility using EDI-OCT (0.945–0.994)[6,18] as well other spectral domain non-EDI OCT instruments.[19] Ikuno et al.[16] reported relatively lower interobserver correlation coefficients (ICCs) (0.6–0.8) using high penetration OCT and EDI-OCT. The cause of this low reproducibility was reported to be manual segmentation and participation of six observers. However, those reports measured choroidal thickness on a single (subfoveal) point or on multiple points on a single scan.

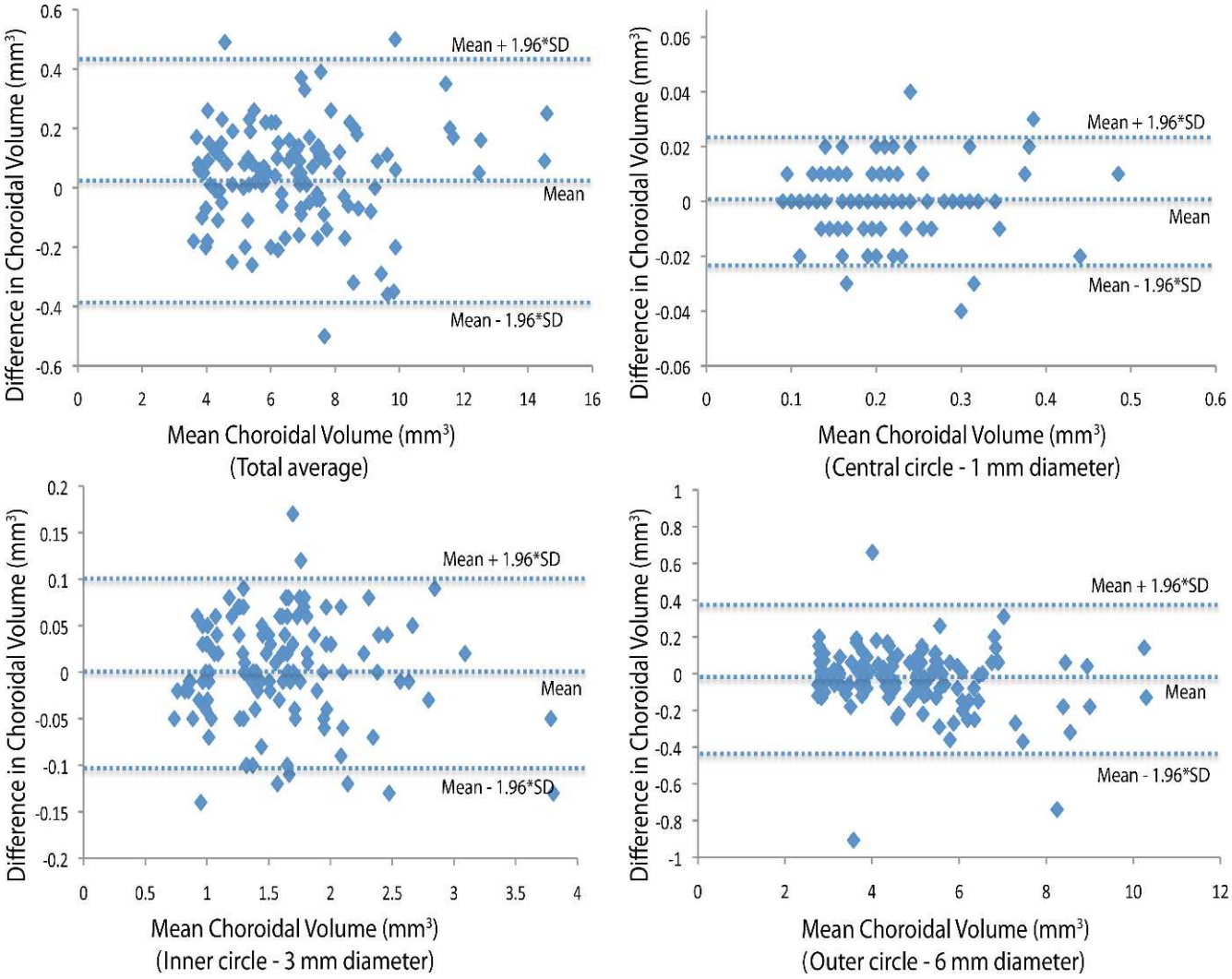

Figure 2. Interobserver reproducibility. Bland-Altman plot of differences relative to mean choroidal volume shows no significant change in interobserver variability for the range of choroidal volume measurements. Dashed lines show mean difference and 95% limits of agreement (1.96 × SD).

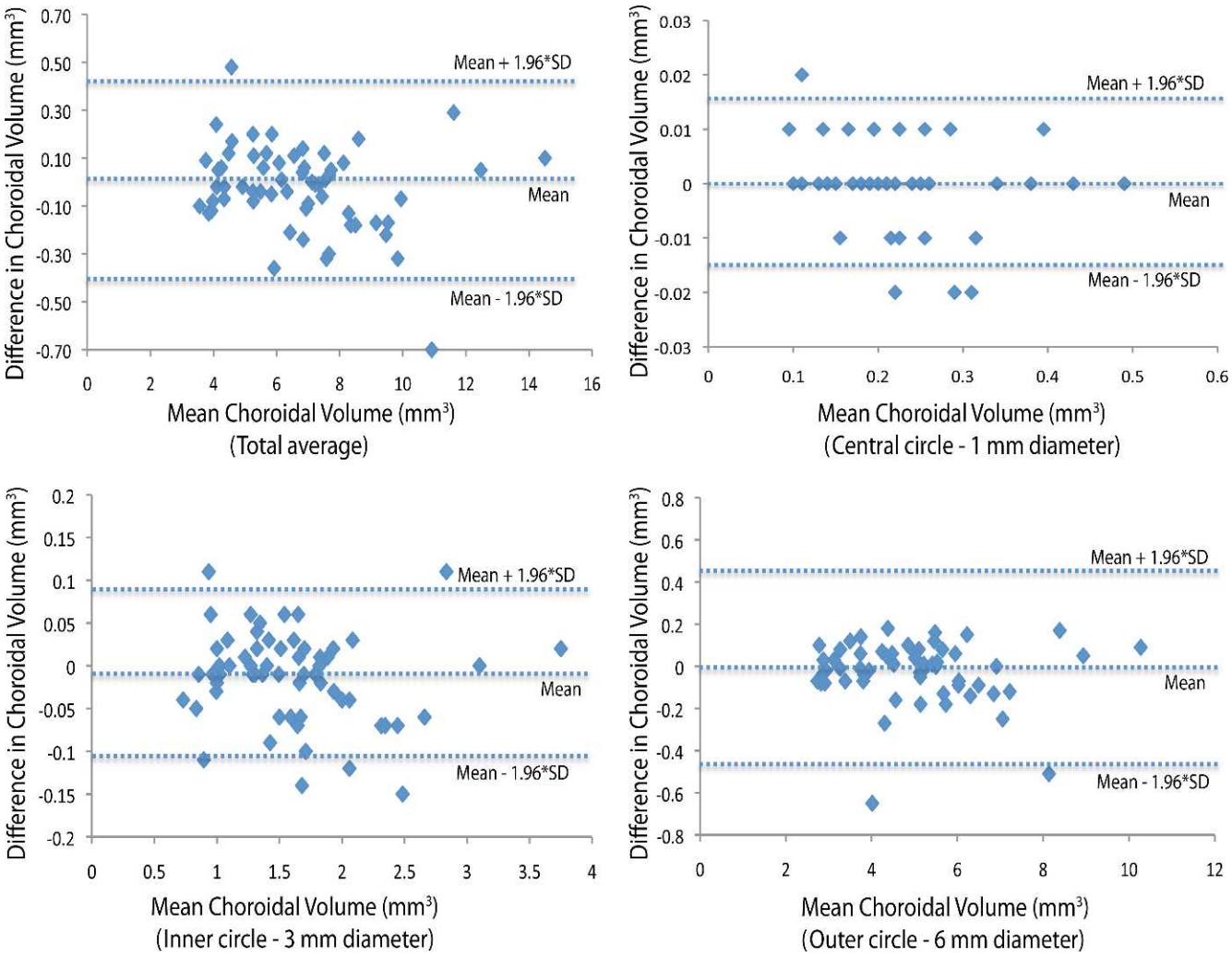

Figure 3. Intraobserver repeatability (Observer 1). Bland-Altman plot of differences relative to mean choroidal volume shows no significant change in intraobserver variability for Observer 1 for the range of choroidal volume measurements. Dashed lines show mean differences and 95% limits of agreement (1.96 × SD).

Recently, a few reports have shown good reproducibility of choroidal volume measurements using long-wavelength OCT devices.[20,21] Shin et al.[25] in a recent study performed choroidal volume measurement using six radial scan protocol on conventional SD-OCT. However, poor visualization of the choroid–sclera junction due to inadequate averaging (eight images) and disproportionate interpolation due to few (six) scans compromised the validity of the measurements. In our study, we used the EDI-OCT on conventional SD-OCT, using built-in automated retinal segmentation software to measure the choroidal volume by manual segmentation at the posterior pole and showed a good reproducibility. Based on these boundaries after manual segmentation, choroidal thicknesses and volumes could be calculated for each of nine standardized subfields with the same software on the same device.

The swept source OCT, not yet approved by the US Food and Drug Administration or the European Medicines Agency (London, UK), has the potential to produce even higher quality choroidal image due to its longer wavelength, potentially higher detection efficiency,[22] and lower dispersion.[23] However, in SD-OCT, it is difficult to maintain high-phase stability.[24] This may be one reason why commercial instruments have not yet become available. Imaging the choroid with an SD-OCT and a 1060-nm light source was recently presented in a research setting.[21] This technology suffers from the lack of a suitable low-cost linear charge-coupled device sensor.[23] Moreover, the EDI-OCT, which we used, gives an excellent quality image with clearly demarcated choroidal borders for quantitative assessment of the choroid. The need for multiple image averaging (approximately 100 images) has been reported as one of the drawbacks of EDI-OCT.[16] However, we observed that the average of 25 to 30 scans was adequate to give a choroidal image with well-demarcated borders in most cases. The number of images for averaging can easily be increased to achieve a good quality choroidal image, especially in cases of difficult visualization of the external border of the choroid due to hyperpigmented outer retinal layers.

We observed that the chorioscleral interface could be irregular or bumpy in different areas in the same eye. Single-point choroidal thickness measurement could therefore be misleading. Choroidal volume quantifies the overall disease burden and could be helpful in understanding the pathophysiology and course and for assessing the response to treatment in chorioretinal disorders.

In conclusion, EDI-OCT can be used to obtain high-quality choroidal images for choroidal thickness and volume measurements including three-dimensional imaging. Choroidal volume measurement by manual segmentation using built-in automat-

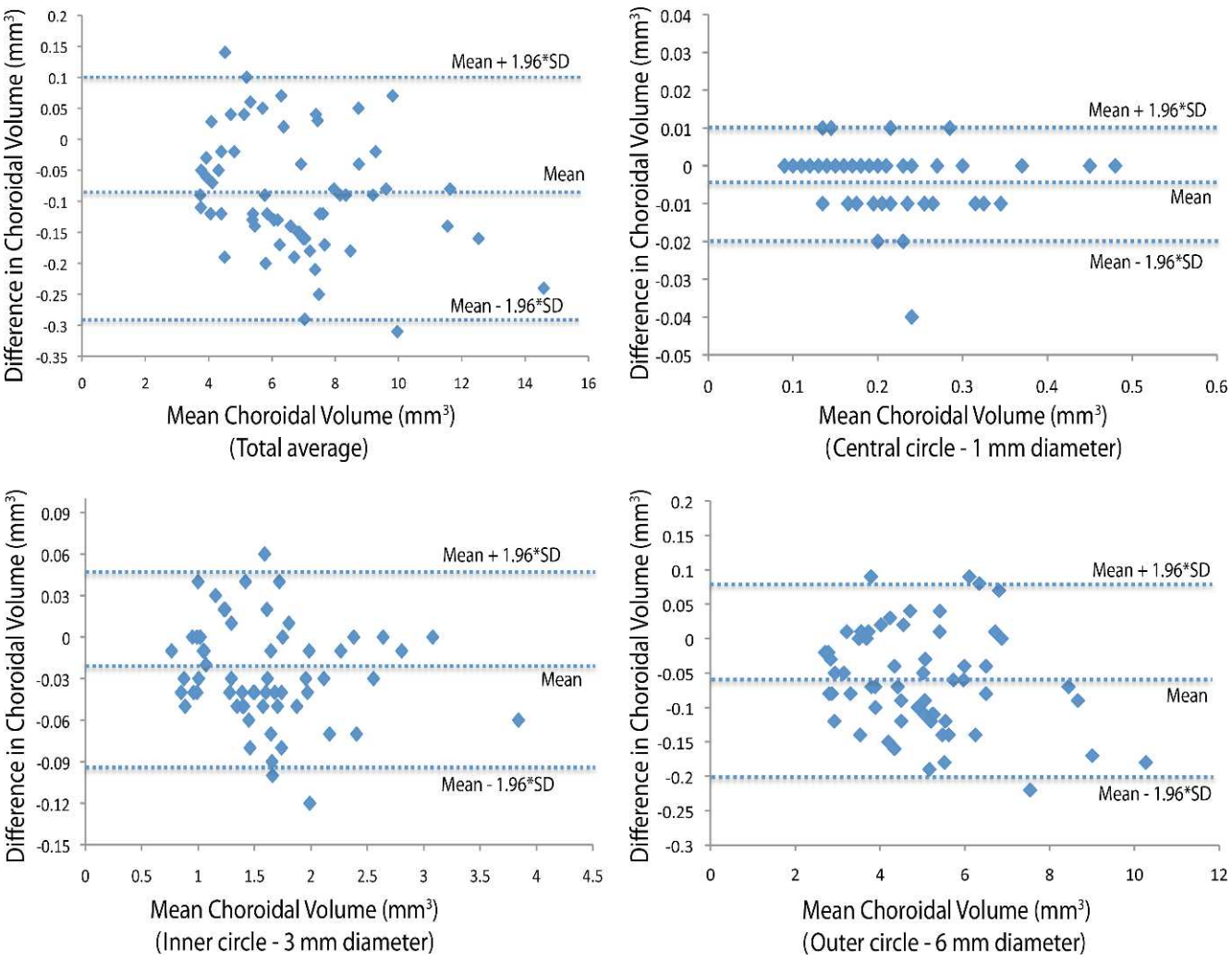

Figure 4. Intraobserver repeatability (Observer 2). Bland-Altman plot of difference relative to mean choroidal volume shows no significant change in intraobserver variability for Observer 2 for the range of choroidal volume measurements. Dashed lines show mean difference and 95% limits of agreement (1.96 × SD).

ed retinal segmentation software on EDI Spectralis OCT is highly reproducible and repeatable and has a very small range of variability. Further studies are required to determine choroidal volume database in normal patients and in different chorioretinal pathologies.

References

1. Ross A, Ross AH, Mohamed Q. Review and update of central serous chorioretinopathy. *Curr Opin Ophthalmol*. 2011;22: 166–173.
2. Yannuzzi LA, Sorenson J, Spaide RF, Lipson B. Idiopathic polypoidal choroidal vasculopathy (IPCV). *Retina*. 1990;10: 1–8.
3. Read RW, Rao NA, Cunningham ET. Vogt-Koyanagi-Harada disease. *Curr Opin Ophthalmol*. 2000;11:437–442.
4. Guyer DR, Puliafito CA, Mones JM, Friedman E, Chang W, Verdooner SR. Digital indocyanine-green angiography in chorioretinal disorders. *Ophthalmology*. 1992;99:287–291.
5. Coleman DJ, Lizzi FL. In vivo choroidal thickness measurement. *Am J Ophthalmol*. 1979;88:369–375.
6. Margolis R, Spaide RF. A pilot study of enhanced depth imaging optical coherence tomography of the choroid in normal eyes. *Am J Ophthalmol*. 2009;147:811–815.
7. Chung SE, Kang SW, Lee JH, Kim YT. Choroidal thickness in polypoidal choroidal vasculopathy and exudative age-related macular degeneration. *Ophthalmology*. 2011;118:840–845.
8. Koizumi H, Yamagishi T, Yamazaki T, Kawasaki R, Kinoshita S. Subfoveal choroidal thickness in typical age-related macular degeneration and polypoidal choroidal vasculopathy. *Graefes Arch Clin Exp Ophthalmol*. 2011;249:1123–1128.
9. Fujiwara T, Imamura Y, Margolis R, Slakter JS, Spaide RF. Enhanced depth imaging optical coherence tomography of the choroid in highly myopic eyes. *Am J Ophthalmol*. 2009;148: 445–450.
10. Imamura Y, Fujiwara T, Margolis R, Spaide RF. Enhanced depth imaging optical coherence tomography of the choroid in central serous chorioretinopathy. *Retina*. 2009;29:1469–1473.
11. Aoyagi R, Hayashi T, Masai A, et al. Subfoveal choroidal thickness in multiple evanescent white dot syndrome. *Clin Exp Optom*. 2012;95:212–217.
12. Fong AH, Li KK, Wong D. Choroidal evaluation using enhanced depth imaging spectral-domain optical coherence tomography in Vogt-Koyanagi-Harada disease. *Retina*. 2011; 31:502–509.
13. Maruko I, Iida T, Sugano Y, et al. Subfoveal choroidal thickness after treatment of Vogt-Koyanagi-Harada disease. *Retina*. 2011; 31:510–517.

14. Grading diabetic retinopathy from stereoscopic color fundus photographs—an extension of the modified Airlie House classification. ETDRS report number 10. *Early Treatment Diabetic Retinopathy Study Research Group. Ophthalmology*. 1991;98:786–806.
15. Bland JM, Altman DG. Statistical methods for assessing agreement between two methods of clinical measurement. *Lancet*. 1986;1:307–310.
16. Ikuno Y, Maruko I, Yasuno Y, et al. Reproducibility of retinal and choroidal thickness measurements in enhanced depth imaging and high-penetration optical coherence tomography. *Invest Ophthalmol Vis Sci*. 2011;52:5536–5540.
17. Rahman W, Chen FK, Yeoh J, Patel P, Tufail A, Da Cruz L. Repeatability of manual subfoveal choroidal thickness measurements in healthy subjects using the technique of enhanced depth imaging optical coherence tomography. *Invest Ophthalmol Vis Sci*. 2011;52:2267–2271.
18. Spaide RF, Koizumi H, Pozzoni MC. Enhanced depth imaging spectral-domain optical coherence tomography. *Am J Ophthalmol*. 2008;146:496–500.
19. Branchini L, Regatieri CV, Flores-Moreno I, Baumann B, Fujimoto JG, Duker JS. Reproducibility of choroidal thickness measurements across three spectral domain optical coherence tomography systems. *Ophthalmology*. 2012;119:119–123.
20. Hirata M, Tsujikawa A, Matsumoto A, et al. Macular choroidal thickness and volume in normal subjects measured by swept-source optical coherence tomography. *Invest Ophthalmol Vis Sci*. 2011;52:4971–4978.
21. Ouyang Y, Heussen FM, Mokwa N, et al. Spatial distribution of posterior pole choroidal thickness by spectral domain optical coherence tomography. *Invest Ophthalmol Vis Sci*. 2011;52:7019–7026.
22. Chinn SR, Swanson EA, Fujimoto JG. Optical coherence tomography using a frequency-tunable optical source. *Opt Lett*. 1997;22:340–342.
23. Yasuno Y, Hong Y, Makita S, et al. In vivo high-contrast imaging of deep posterior eye by 1-microm swept source optical coherence tomography and scattering optical coherence angiography. *Opt Express*. 2007;15:6121–6139.
24. Zhang J, Chen Z. In vivo blood flow imaging by a swept laser source based Fourier domain optical Doppler tomography. *Opt Express*. 2005;13:7449–7457.
25. Shin JW, Shin YU, Lee BR. Choroidal thickness and volume mapping by a six radial scan protocol on spectral-domain optical coherence tomography. *Ophthalmology*. 2012 Jan 24. [Epub ahead of print]